Electromagnetic bias estimates based on TOPEX, buoy, and wave model data

Raj Kumar
Oceanic Sciences Division, MOG/RESA, Space Applications Centre (ISRO), Ahmedabad, India

Detlef Stammer and W. Kendall Melville
Scripps Institution of Oceanography, La Jolla, California, USA

Peter Janssen
European Centre for Medium-Range Weather Forecasts, Reading, UK

Received 8 July 2002; revised 1 July 2003; accepted 7 August 2003; published 13 November 2003.

[1] For quantitative studies of the ocean using altimetric measurements, the sea surface height measurements must be corrected for the electromagnetic (EM) bias effect. Project-provided EM bias correction algorithms were derived from the altimeter data as a function of wind speed and wave height through variance minimization techniques [*Gaspar et al.*, 1994]. In this paper we characterize the impact of those corrections on the altimeter data and compare it with an empirical algorithm based on tower observations of wave slopes and wave age (W. K. Melville et al., Wave slope and wave age effects in measurements of EM bias, submitted to *Journal of Geophysical Research*, 2002) and with theoretical predictions of EM bias [*Srokosz*, 1986]. We find a significant correlation between high-frequency ocean signals with the project-provided EM bias correction. This suggests that an EM bias algorithm cannot be estimated from altimeter data alone through variance minimization techniques. Since the EM bias depends on parameters that cannot be measured by an altimeter (e.g., wave slope), improved theoretical corrections appear to be preferable to altimetry-based empirical estimates. Using wave buoy and wave model (WAM) data, we find good agreement between existing theoretical correction and empirical corrections based on wave slope and wave age information over a significant range of parameters. Although further work is needed to extend our tests of algorithms to larger wave slopes, existing wave slope and wave age-based algorithms appear comparable in goodness to project-provided empirical algorithms and may be used for routine altimetry processing in combination with WAM output on a global basis. *INDEX TERMS:* 4275 Oceanography: General: Remote sensing and electromagnetic processes (0689); 4294 Oceanography: General: Instruments and techniques; 4504 Oceanography: Physical: Air/sea interactions (0312); 4532 Oceanography: Physical: General circulation; *KEYWORDS:* EM bias, altimetry, barotropic circulation, remote sensing

Citation: Kumar, R., D. Stammer, W. K. Melville, and P. Janssen, Electromagnetic bias estimates based on TOPEX, buoy, and wave model data, *J. Geophys. Res.*, *108*(C11), 3351, doi:10.1029/2002JC001525, 2003.

1. Introduction

[2] For quantitative studies of the ocean circulation, altimetric measurements must be corrected for several atmospheric and geophysical effects. One of those corrections is for the so-called sea state bias, which consists of two terms: an electromagnetic (EM) bias and a skewness bias. For TOPEX/Poseidon (T/P) data the latter is part of the ground-based processing, assuming a constant value (0.1) for the skewness (see *Hayne et al.* [1994] for details). Of primary concern for scientific applications of T/P data is the EM bias term and its uncertainty (but see below for a more general discussion). *Chelton et al.* [2001] give a recent review of the status of the electromagnetic bias estimates and refer to this correction as one of the largest remaining uncertainties in altimeter data.

[3] The physical basis for the EM bias is well established: because of a greater backscatter per unit surface area from wave troughs than from wave crests, the EM measurement of the sea surface height (SSH) is biased low when compared to the mean sea surface. Since the first studies by *Yaplee et al.* [1971], observations have revealed the primary scaling of the EM bias correction, ϵ, on the significant wave height $H_{1/3}$, usually expressed as

$$\epsilon = -\beta H_{1/3}. \quad (1)$$

0148-0227/03/2002JC001525$09.00

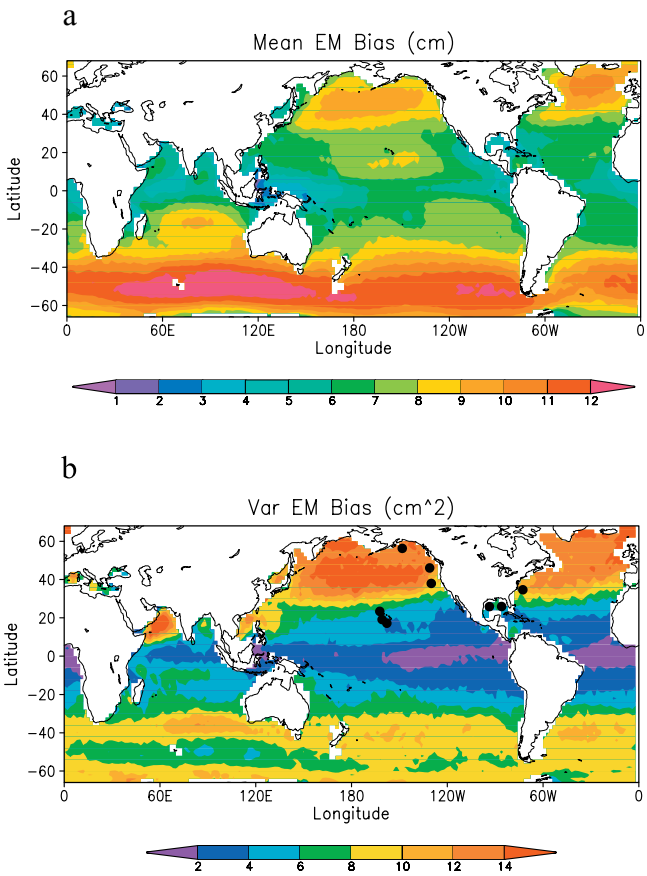

Figure 1. (a) Mean (in cm) and (b) STD^2 (in cm^2) of the EM bias correction, computed from 8 years of T/P data according to equation (1) with β given by equation (2). Black dots show the locations of the buoys listed in Table 1.

The coefficient β describes a nondimensional proportionality factor which is roughly a few percent of $H_{1/3}$. Tower and aircraft data have shown the additional dependence of β on the RADAR frequency and wind speed, among others [*Melville et al.*, 1991; *Hevizi et al.*, 1993; *Arnold et al.*, 1995], rendering it a complicated and not well understood multivariate function. An additional complicating factor in determining this correction from observations is the fact that EM bias algorithms estimated from aircraft and tower-based measurements are not necessarily applicable to spaceborne altimeter data, since the radar return from a distant target may be significantly different from a small tower-based footprint. Yet, satellite data have indicated an approximately similar parameter dependence as was found from the aircraft and tower-based observations [*Ray and Koblinsky*, 1991; *Millet et al.*, 2003b; *Gaspar et al.*, 2002].

[4] Many of the empirical and theoretical approaches over the last several years consisted of efforts to determine the exact dependence of β on parameters such as wave height, wind speed, or wave age. Among them, *Gaspar et al.* [1994] derived a parametric relation between β and wind speed U and $H_{1/3}$ from T/P data by minimizing the sea surface height (SSH) variability, globally, in space and time from crossover differences. They obtained the best results using a four parameter model

$$\beta = \alpha_0 + \alpha_1 U + \alpha_2 U^2 + \alpha_3 H_{1/3}. \quad (2)$$

The accuracy of this empirical EM bias parameterization is specified as 1.5 cm for the time-varying part, but several times that amplitude for the time mean component [see also *Chelton et al.*, 2001]. A slightly better correction, resulting from a more recent nonparametric approach [*Gaspar and Florens*, 1998], appears accurate to about 1 cm.

[5] Using nadir Doppler microwave measurements from a platform in Bass Strait, Melville et al. (submitted manuscript, 2002) demonstrated a significantly better correlation between the dimensionless EM bias, β, and both the dimensionless wave slope and wave age than can be obtained with the traditional dimensional variables, wind speed and wave height. It was found that the residual root mean square (RMS) error in the correction could be reduced by up to 50% when the dimensionless variables were used. This improvement was relatively insensitive to whether parametric or optimal estimation (objective mapping) techniques were used to fit the data. The rationale for the use of both wave slope and wave age as independent variables can be based on a dimensional analysis as well as on the existence of long-wave-short-wave interaction models in which the wave slope is the relevant long-wave expansion parameter in the limit of very short waves on longer waves. Because required input fields (wave slope and wave age) are not measured along with altimetric observations, this parameterization of EM bias has not been tested with altimeter data previously.

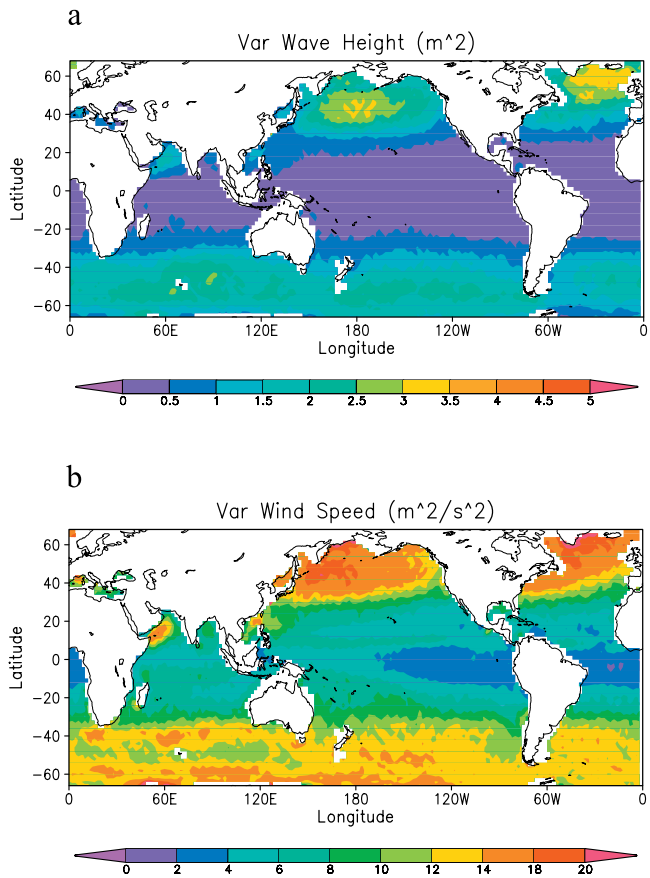

Figure 2. STD^2 of (a) wave height (in m^2) and (b) wind speed fields (in m^2/s^2) computed from 8 years of T/P data.

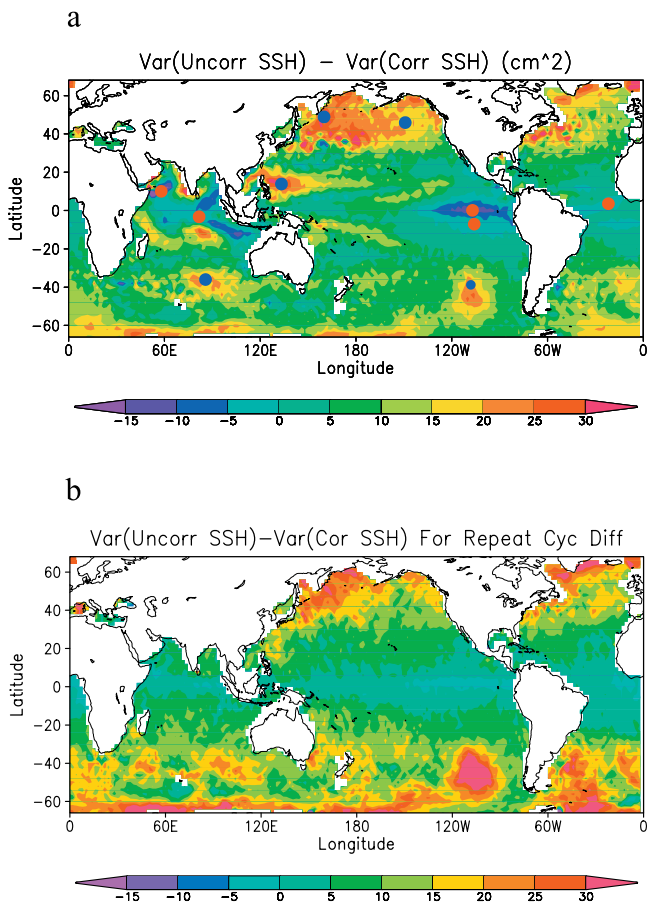

Figure 3. (a) Difference of SSH variability (in cm^2) without minus with the EM bias correction applied. Positive values indicate a reduction in SSH variance resulting from the EM bias correction. Red and blue dots mark the position from which spectra are being shown in Figures 5b and 5c, respectively. (b) Similar difference field, but for variability of η', i.e., 10-day differences in SSH, without and with EM bias correction applied (in cm^2).

[6] The purpose of this paper is twofold. In its first part we will for the first time investigate the space-time characteristics of the project-provided EM bias correction and study its impact on the altimetric SSH data. As will become clear below, the effect is not always as expected. Instead we will show indications that the empirical altimeter data-based correction does also remove some high-frequency ocean variability from the observations. To overcome the problem of overcorrection and thereby to help improving the altimetric data quality, we investigate therefore subsequently the applicability of the tower-based Melville et al. (submitted manuscript, 2002) parameterization of EM bias to the altimeter data and compare it with the EM bias algorithm for *Gaspar et al.* [1994] and with the theoretical approach from *Srokosz* [1986] (*Elfouhaily et al.* [2001] provides an alternative theoretical approach, and both are discussed in detail by *Gommenginger et al.* [2003]).

[7] Although this will be done in this paper primarily at a few buoy locations where wind and wave data are available simultaneous to T/P altimetry, the long-term goal is to obtain a globally applicable wave slope and age-based EM bias algorithms. However, since simultaneous remote sensing of SSH, wave slopes, and wave age is not possible at present, to apply this algorithm globally, one has to depend upon information available from wave models and in situ data. To test the applicability of output from existing wave models for the EM bias algorithm, we will therefore show here also a comparison of WAM-based results with those obtained from buoy data. Our conclusion is that at the buoy locations, the WAM-based corrections are close to those based on the buoy data suggesting that WAM-based corrections should be a valuable alternative to project-provided EM bias correction that are not contaminated by ocean signal.

[8] We begin our discussion in section 2 with a review of the impact of the EM bias correction on SSH data and study the space-time characteristics of the EM bias term. In section 3 we will then test the Melville et al. (submitted manuscript, 2002) algorithm at buoy locations with altim-

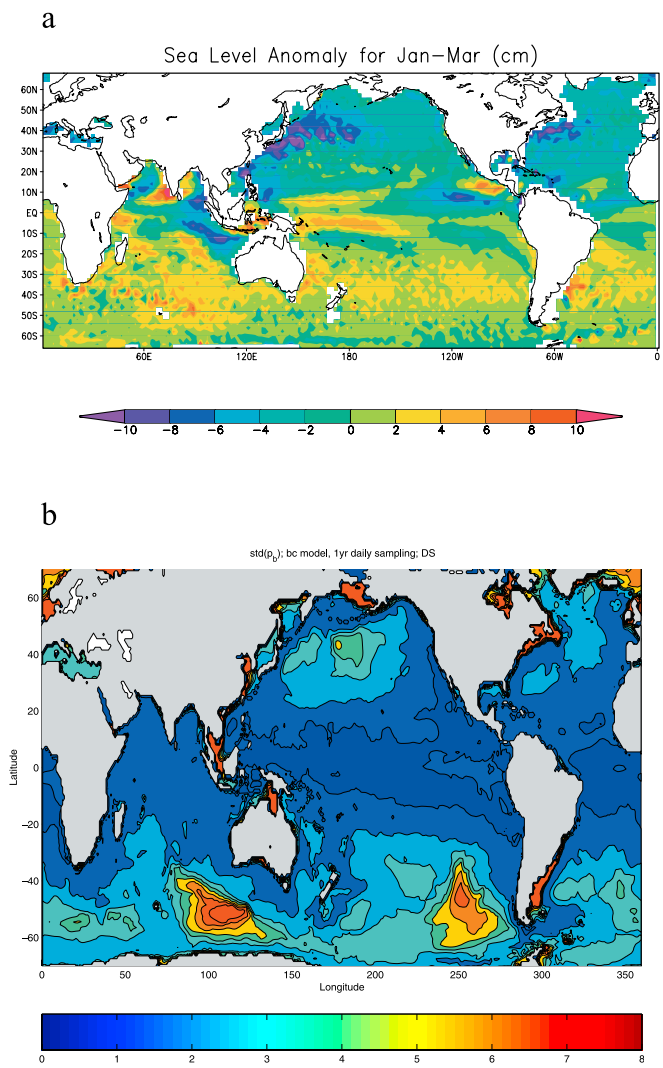

Figure 4. (a) Winter (January–March) mean SSH anomalies, estimated from 8 years of T/P data (1992–2000). (b) Barotropic SSH variability, simulated using a barotropic ocean circulation model driven by twice daily NCEP surface wind stress. The figure is taken from *Stammer et al.* [2000], who provide details on this computation.

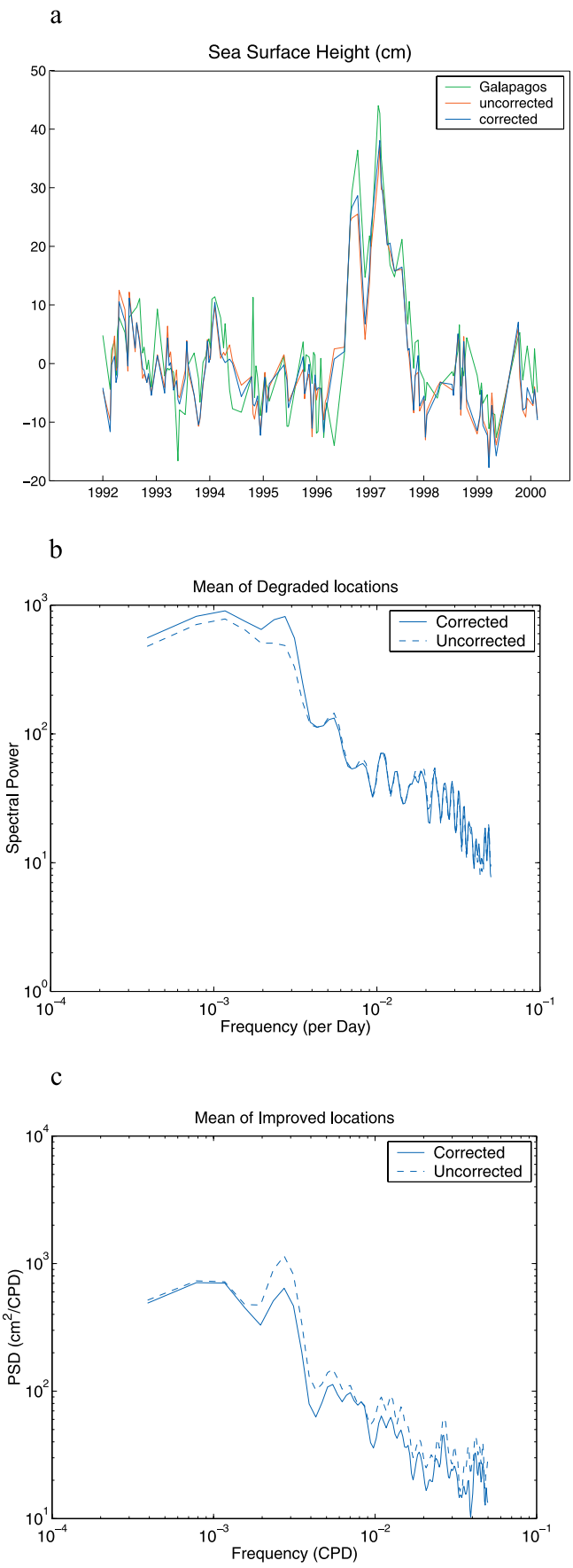

Figure 5. (opposite) (a) Comparison of T/P SSH time series that were corrected (blue) and uncorrected (red) for EM bias effects, with the Santa Cruz tide gauge record (green). Units are centimeters and a temporal mean was removed from each time series. See text for details. Power spectral density (PSD) functions of T/P SSH time series taken from locations marked in Figure 3a as regions with (b) enhanced and (c) reduced SSH variance after applying the EM bias correction. Dashed and solid curves represent SSH records before and after applying the EM bias correction, respectively.

eter data. In section 4 we discuss similar results based on WAM model output. We draw conclusions in section 5.

2. EM Bias Space-Time Characteristics

[9] To assess the importance of the EM bias correction for the quality of T/P data, we start with an analysis of the project-provided correction of the SSH variability inferred from T/P data from the period 1992 through 2000. The altimeter data were processed as described by *Stammer and Wunsch* [1994] with the additional correction of instrumental drifts and offsets between the side A and side B altimeters. No further attempt was made to correct for potentially remaining statistical differences between those two altimeter components. From the results that follow no indication was given that this assumption is invalid (compare Figure 6).

[10] Fields of the mean and STD of the EM bias correction, computed from 8 years of T/P data according to equation (1) with β given by equation (2), are shown in Figure 1. The mean correction has maximum amplitudes around 10 cm in the Southern Ocean; that is, the drop in SSH across the Antarctic Circumpolar Current (ACC) would be seen by an altimeter as roughly 10 cm larger than a true reduction in SSH. We note that this value is of the same amplitude as geoid uncertainties on comparable spatial scales and corresponds to about 5% of the drop in the SSH across the ACC (or equivalently an error of approximately 1 cm/s in velocity). Similar biases are visible in the subpolar basins of the Northern Hemisphere, yet with less dramatic amplitudes.

[11] For the time-varying correction, maximum amplitudes are found over the Northern Hemisphere where strong winter storm events with maximum wind speeds and wave heights are present (see Figure 2). In contrast, the Southern Ocean shows surprisingly small temporal changes in the EM bias term (here wind and waves are year-round high). We note especially the local minimum in the variability of the EM bias correction over the ACC.

[12] In Figure 3 we display the reduction in the variance of the SSH variability from the application of the *Gaspar et al.* [1994] EM bias correction provided by equation (2). Positive values indicate a reduction in SSH variability through the EM bias correction. Several surprising findings can be summarized from the figure.

[13] 1. The variance reduction of the SSH through the application of the EM bias term is relatively modest globally from 92 cm^2 to 83 cm^2, i.e., a decrease of only 9 cm^2. Regionally, the reduction in the SSH variance is in

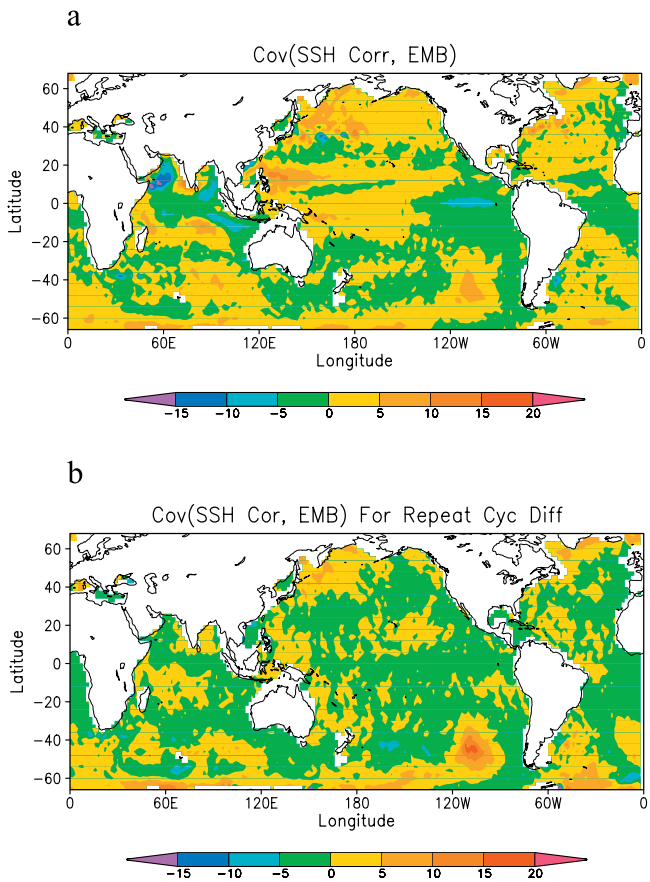

Figure 6. (a) Covariances between the corrected SSH and the EM bias term computed from 8 years of T/P data. (b) Same as in Figure 6a but for differences in the corrected SSH and EM bias term between repeat cycles. Units are cm^2 in both panels.

the range of 5–10 cm^2 and reaches values around 20cm^2 cm only in high latitudes of the Northern Hemisphere or near Antarctica.

[14] 2. There are low-latitude regions in which the SSH variability, instead of decreasing, actually increases upon the application of the EM bias correction, notably the tropical Pacific and Indian Oceans. These changes are significant and reach variance enhancements of up to 15 cm^2 in the Arabian Sea. Since the *Gaspar et al.* [1994] algorithm was derived by obtaining a global minimum in SSH differences at crossover locations, it is not surprising that a few regions would be degraded. What is surprising, however, is that (1) the variance increase has about the same magnitude as the decrease in other regions, (2) these regions are significant in their spatial extent, and (3) the pattern in these negative correction amplitude (increased variance) regions are unlike those in the EM bias correction, wave height, or wind speed fields. Instead, they seem to reflect ocean current structures, especially in the Indian Ocean. We note that T/P SSH anomalies during winter months (not shown) have spatial patterns that are almost identical to those showing increased variability in Figure 3 (compare Figure 4).

[15] For reasons similar to those observed here, *Gaspar and Florens* [1998] have already suggested that EM bias corrections are not appropriate for the tropical regions. However, the increase in variability alone is not an indication that the applied EM bias correction is not valid. To shed further light on the validity of the EM bias correction in those regions, we use tide gauge data available at several locations in the regions showing increased variability. A typical comparison is provided in Figure 5a showing a time series of the Santa Cruz tide gauge on Galapagos Island together with the uncorrected and corrected T/P time series at a nearby location. Despite high-frequency differences in the time series pointing to small-scale signals due to local island or harbor effects in the tide gauge data (see *Mitchum* [1994] for more details), a general tendency of the correction to move T/P data closer toward the tide gauge data is apparent. The RMS difference between tide gauge data and T/P data decreased from 5.47 to 4.85 cm while the RMS variability of SSH increased from 10 to 10.42 cm upon application of the correction which has to be compared to 11.15 cm from the tide gauge record.

[16] Using time series from several tide gauges and nearby altimeter records, we computed power spectral density (PSD) functions of T/P SSH time series taken from those locations marked in Figure 3a as regions with reduced and enhanced SSH variance after applying the EM bias correction. All those regions with increased variability show basically no impact of the EM bias correction on periods shorter than about a year, but a clear increase in power on periods of about a year and longer (Figure 5b). In contrast,

Table 1. Summary Buoy Information[a]

Buoy ID	Longitude, deg	Latitude, deg	Dist, m	Depth, m	Period	Instrument	Data Gaps
41001	287.36	34.68	0.381	4389	10/92–12/2000	6N DACT	12/92–2/93,12/97–6/98,1/2000–5/2000
42002	266.43	25.89	0.402	3200	10/92–12/2000	10D MARS	1/99–2/99
42003	274.09	25.94	0.380	3164	10/92–12/2000	10D MARS	9/94–12/94,10/96–4/97
46001	211.82	56.29	0.292	4206	10/92–12/2000	6N DACT	1/96–4/96
46005	229.00	46.08	0.492	2853	10/92–12/2000	12D DACT	4/93–6/93
46059	230.00	37.98	0.156	4599	10/94–12/2000	6N DACT	
51001	197.73	23.40	0.477	3257	10/92–12/2000	6N GSBP	4/94–5–94,8/94–11/94,4/96–5/96
51002	202.17	17.19	0.470	5002	10/92–12/2000	6N VEEP,MARS	2/93–5/93,4/95–5/95
51003	199.19	19.14	0.141	4883	10/92–11/2000	6N GSBP	

[a]The left column lists the buoy ID number; geographic positions follow in the next two columns for longitude and latitude, respectively; the distance between the buoy and the nearest T/P measurements are listed in column 4; column 5 lists the local water depth; and data period and specifics about the buoy payload and about data gaps are provided in the three rightmost columns.

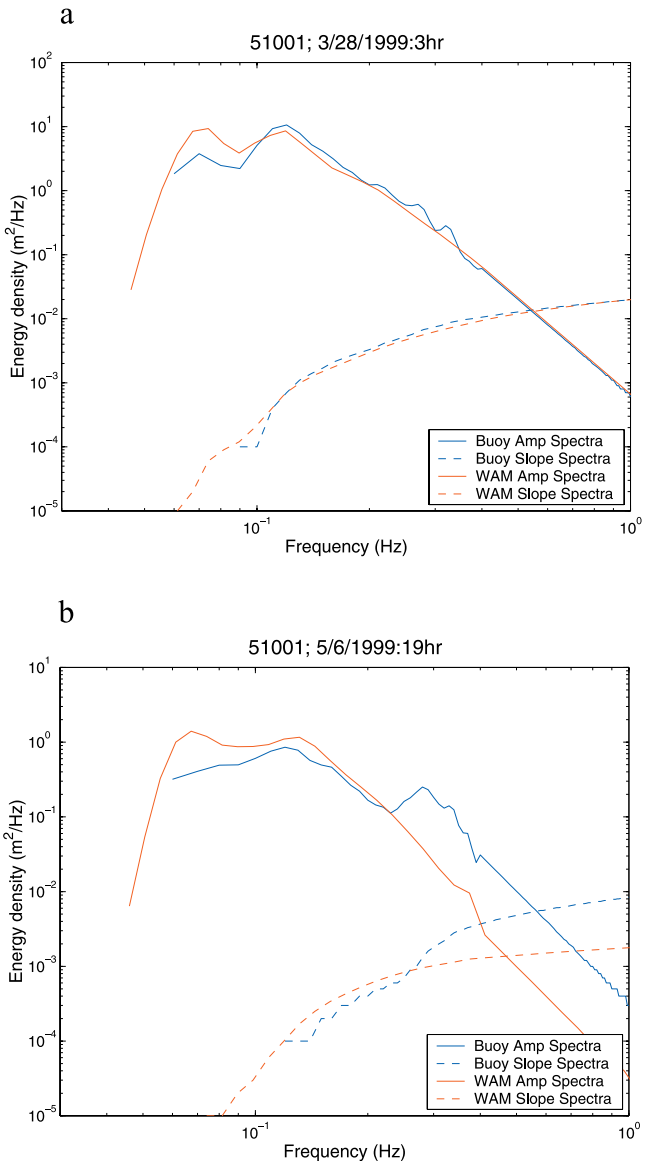

Figure 7. Typical wave elevation (solid curves) and wave slope spectra (dashed curves) for (top) 28 March 1999 and (bottom) 6 May 1999 at the location of buoy 51001 (197.73°E, 23.4°N). Shown are results from buoy data (blue) and from WAM output (red). See text for details.

at all locations with reduced SSH variance, SSH power decreases on roughly all periods shorter than a year (Figure 5c).

[17] Figure 5 strongly suggests that using a global minimum in SSH variability as a basis for judging the quality of an EM bias correction will not be the appropriate measure of goodness but that absolute SSH time series from tide gauge stations or other measurement sites are required for a quantitative test, contrary to past practices. Moreover, a frequency-dependent minimization of the SSH variability will be required to determine an EM bias parameterization. In this regard, we note that *Gaspar et al.* [1994] in fact did minimize SSH differences at crossover positions, thus concentrating on periods shorter than 8 days (maximum time lag at cross overs is around ±5 days). From Figure 5 it seems that the resulting correction works in the sense that it shifts the SSH data closer to tide gauge records, despite the fact that the SSH variance is being increased at the same time.

[18] For a further comparison with results from *Gaspar et al.* [1994] we show in Figure 3b the reduction in variability of SSH differences, $\eta' = \eta_{i+1} - \eta_i$, between repeat cycles i and $i + 1$, thus focusing the discussion on the effect of the EM bias correction on high-frequency SSH signals. The global variance of the SSH differences reduces from 99 cm^2 to 89 cm^2, i.e., by 10 cm^2, in good agreement with results from *Gaspar and Florens* [1998]. Quite clearly, the effect of the correction on SSH differences is about zero in low latitudes where the negative impact essentially disappeared. Enhanced variance reduction is now limited to high latitudes. However, the spatial pattern of the reduction warrants a further discussion.

[19] Generally an altimeter measures a sum of the true SSH, η_t, and the EM bias term, η_{em} (neglecting all other environmental and geophysical effects), i.e.,

$$\eta = \eta_t + \eta_{em}. \tag{3}$$

Accordingly, the following holds for the variances

$$\langle \eta^2 \rangle - \langle \eta_t^2 \rangle = \langle \eta_{em}^2 \rangle + \langle 2\eta_t \eta_{em} \rangle, \tag{4}$$

where the angle brackets denote the relevant averaging, with a similar equation describing variances of the SSH differences. The left-hand side of equation (4) was displayed in Figure 3 for both SSH and SSH differences. The first term on the right hand side is displayed in Figure 1b. The second term on the right hand side, i.e., the local covariance between η_t and η_{em}, is displayed in Figure 6. It is assumed to be zero globally, when the EM bias correction is determined through a variance minimization of SSH or SSH differences. In contrast, we find it locally to be of the same order of magnitude as the $\langle \eta_{em}^2 \rangle$ term. Moreover it is responsible for the regional pattern visible in Figure 3. A comparison with Figure 3b reveals a striking resemblance of this pattern with regions of enhanced barotropic variability [see also *Ponte and Gaspar*, 1999, Plates 1–3]. This suggests that the empirical *Gaspar et al.* [1994] algorithm removes not only EM bias effects but in fact might also remove high-frequency ocean signal. It was suggested previously by *Gaspar and Florens* [1998] that the EM bias fit needs to be done jointly with an estimate of the ionospheric correction. Here there seems to be evidence that the barotropic energy needs to be accounted for in the estimation procedure as well. Therefore one might generally conclude that theory-based or altimeter-independent EM bias corrections should be superior to empirical altimeter corrections since they avoid these problems.

[20] It is noteworthy that the *Gaspar et al.* [1994] EM bias algorithm removed more variance from the SSH observations than would be achieved by using a simple, fixed, 2% of SWH as a measure of the EM bias effect. However, most of the excess variance is actually removed in those regions with enhanced covariance between the corrected SSH variability (mostly barotropic) and the EM bias

Table 2. Standard Deviation of SSH at Buoy Locations[a]

Buoy ID	Longitude, deg	Latitude, deg	Distance, m	No Pts		STD, cm			Var Diff, cm^2	
				0.2	0.12	Orig	Gasp	Buoy	0.2	0.12
41001	287.36	34.68	0.381	194	140	19.7	18.9	18.6	10.3	10.8
42002	266.43	25.89	0.402	243	112	16.8	16.3	16.1	5.0	4.3
42003	274.09	25.94	0.380	197	165	26.1	26.1	26.2	−2.7	4.9
46001	211.82	56.29	0.292	250	122	9.0	8.0	7.9	1.5	4.3
46005	229.00	46.08	0.492	33	20	7.3	5.5	5.1	4.5	−2.2
46059	230.00	37.98	0.156	206	158	9.4	8.9	9.2	−3.9	−3.3
51001	197.73	23.40	0.477	217	106	9.1	8.8	8.8	−1.6	1.0
51002	202.17	17.19	0.470	250	84	7.5	7.0	7.1	−1.6	0.4
51003	199.19	19.14	0.141	259	189	10.1	9.9	10.0	−2.3	−2.4

[a]Columns 5 and 6 list the number of valid data points used for the comparison. Columns 7–9 list the SSH standard deviation obtained without EM bias correction and when applying the *Gaspar et al.* [1994] and the Melville et al. (submitted manuscript, 2002) parameters. The last two columns show the reduction in SSH variance using the Melville et al. (submitted manuscript, 2002) algorithm as opposed to the *Gaspar et al.* [1994] algorithm. Positive values indicate an improvement (in cm^2). In the last but one column, slope values up to 0.2 were used. In the last column, slope value only up to 0.12 were used.

term. We note also that the low latitudes do not show enhanced variances when using the simple SWH-based correction.

[21] To summarize, variance reduction is not a sufficient measure of goodness of a EM bias correction algorithm. Especially, altimeter data-based empirical corrections seem to be contaminated by high-frequency ocean signal. Instead one needs to seek alternative algorithm that use independent information, but also can produce corrections on a global basis and simultaneous to altimetric measurements. Wave slope and wave age-based corrections come to mind that can be used in conjunction with output from WAM models. We will therefore in the following test those algorithms using information from buoys and then show their applicability using WAM output.

3. Testing a Wave Slope-Based EM Bias Algorithm

[22] To investigate the applicability of the Melville et al. (submitted manuscript, 2002) EM bias algorithm to T/P data, we used wave observations from the 9 buoys at the locations shown in Figure 1. Data were obtained from NOAA (see http://www.nodc.noaa.gov). See Table 1 for details about the source of the buoy data, their availability during the period 1992 through 2000, specifics of the instrument hardware, as well as the parameters measured. Nearest T/P data from within 50 km distance of the buoy location were compared to buoy observations that in turn were taken within ±1h of a T/P overflight.

[23] At the buoy locations, surface wave frequency spectra ϕ are available which generally contain contributions from wind sea and swell. A typical example is given in Figure 7 from buoy 51001 located at 197.7°E, 23.4°N in the Pacific. In this example, the wind sea peaks at a frequency of 0.12 Hz. A secondary peak near 0.07 Hz is due to swell. Processes that are responsible for the sea state bias are dependent on the slope of the waves that are longer than the scale of the primary scatterering surfaces, in a two-scale model. Since the slope spectrum is proportional to k^2 times the wave spectrum, this weights the slope spectrum toward shorter waves. In the absence of anomalous conditions, the longer swell waves contribute therefore little to the slope and relevant for an EM bias correction is primarily the wind-sea component.

[24] Also shown in the figure is the corresponding slope spectrum. To compute it from the wave spectrum, we used a deepwater linear dispersion relation to compute the wave number

$$k = \frac{2\pi f^2}{g}. \tag{5}$$

With this relation, the slope spectrum, $S(f_i)$, and the RMS slope, s_l, may be estimated [e.g., *Cox and Munk*, 1956] as

$$S(f_i) = \frac{(2\pi f_i)^4}{g^2}\Phi(f_i), \tag{6}$$

$$s_l = \left[\sum_{i=1}^{N} f_s S(f_i)\right]^{1/2}, \tag{7}$$

where f_s is the fundamental frequency (i.e., the 1/T, where T is the length of the time series) and $\Phi(fi)$ is surface height displacement spectrum.

Table 3. Standard Deviation of SSH Differences at Buoy Locations Between Successive Repeat Cycles for Slopes up to 0.2[a]

Buoy ID	Longitude, deg	Latitude, deg	Distance, m	No Pts	STD, cm			Var Diff, cm^2
					Orig	Gasp	Buoy	Buoy
41001	287.36	34.68	0.381	30	9.8	10.0	10.7	−14.6
42002	266.43	25.89	0.402	24	7.1	7.0	6.3	7.1
42002	266.43	25.89	0.402	22	9.8	9.1	8.9	14.4
46001	211.82	56.29	0.292	24	9.7	6.5	5.3	−12.4
51001	197.73	23.40	0.477	28	9.4	9.3	9.5	−11.4
51002	202.17	17.19	0.470	40	6.4	5.4	5.5	−1.0
51003	199.19	19.14	0.141	27	7.3	6.4	6.3	2.0

[a]Column 5 lists the number of valid data pairs used. Columns 6–8 list the standard deviation of SSH differences obtained without EM bias correction and when applying the *Gaspar et al.* [1994] and the Melville et al. (submitted manuscript, 2002) parameters. The last column shows the reduction in SSH variance using the Melville et al. (submitted manuscript, 2002) algorithm as opposed to the *Gaspar et al.* [1994] algorithm. Positive values indicate an improvement (in cm^2).

Table 4. Standard Deviation of SSH at Buoy Locations Using Buoy Data and WAM Output[a]

Buoy ID	Longitude, deg	Latitude, deg	Distance, m	No Pts		SSH STD, cm				Var Diff, cm^2			
				0.2	0.12	Orig	Gasp	Buoy	WAM	MBuoy	MWAM	GBuoy	GWAM
41001	287.36	34.68	0.381	45	35	21.2	21.1	21.0	20.8	4.9	13.9	9.4	28.4
42002	266.43	25.89	0.402	56	53	15.0	14.3	14.1	14.4	4.6	−3.1	0.2	−1.6
42003	274.09	25.94	0.380	61	52	26.5	26.3	26.5	26.6	−10.4	−17.5	−0.6	−21.3
46001	211.82	56.29	0.292	56	37	8.2	7.5	7.4	7.8	1.7	−5.2	1.2	−3.9
46005	229.00	46.08	0.492	23	16	7.5	5.5	4.9	5.5	7.0	0.7	−1.7	−2.3
46059	230.00	37.98	0.156	58	48	10.2	9.5	9.4	10.0	1.4	−10.1	1.8	−11.8
51001	197.73	23.40	0.477	56	30	7.2	7.1	7.3	7.2	−3.1	−2.4	−3.9	−2.7
51002	202.17	17.19	0.470	46	17	5.9	6.1	6.2	6.6	−1.1	−6.7	−5.0	−5.4
51003	199.19	19.14	0.141	70	55	10.7	10.4	10.3	10.6	2.8	−3.7	2.8	−2.5

[a]Columns 5 and 6 list the number of valid data points used for the comparison. Columns 7–10 list the SSH standard deviation obtained without EM bias correction, when applying the *Gaspar et al.* [1994] algorithm and the Melville et al. (submitted manuscript, 2002) algorithm separately for buoy data and WAM output. The last four columns show the reduction in SSH variance using the Melville et al. (submitted manuscript, 2002) (M) algorithm as opposed to the *Gaspar et al.* [1994] (G) algorithm separately for buoy data and WAM output. Positive values indicate an improvement (in cm^2). In columns 11–12, slope values up to 0.2 were used. In the last two columns, slope value only up to 0.12 were used.

[25] To compute wave ages at the buoy locations, wave phase speeds have been computed using the dispersion relation

$$c_p = \sqrt{g/k_p} \tag{8}$$

where k_p is provided as a peak wind-sea wave number (we recall that only the wind sea component of the spectrum is the relevant part for this computation; see above). The wave age was then computed from the ratio of c_p and wind speed, using wind speed U_{10} measurements from the T/P altimeter records.

[26] The Melville et al. (submitted manuscript, 2002) algorithm was developed from measurements made in Bass Strait at wave frequencies up to 1.0 Hz and is available in form of a polynomial for the normalized bias coefficient

$$\beta = -0.45 + 36.3 s_p + 293.9 s_p^2 - 2331.0 s_p^3 + 0.2447\left(u_{10}/c_p\right) + 0.3526\left(u_{10}/c_p\right)^2 - 0.2302\left(u_{10}/c_p\right)^3. \tag{9}$$

The dimensional EM bias correction then follows from equation (1). Because the buoy data available to us only cover the frequency range from 0.04–0.4 Hz, some extrapolation is necessary to make the above Melville et al. (submitted manuscript, 2002) polynomial applicable to the buoy data. For this purpose, we extended our data set from 0.4 Hz up to 1 Hz using a f^{-5} tail [*Komen et al.*, 1994]. A slope spectrum was computed subsequently from the extended spectrum, using equation (6).

[27] In Table 2 we compare the impact of the respective EM bias correction on the SSH variability with that resulting from the *Gaspar et al.* [1994] algorithm at the buoy locations. At almost all buoy locations the SSH variability does decrease through the EM bias correction. However, results are consistent with our previous finding in that the respective RMS variance reduction is only in the cm range. Changes in the SSH variance due to the use of the two different EM bias algorithms are in the range of 1–10 cm^2, and are mostly positive, indicating a larger SSH variance reduction through the Melville et al. (submitted manuscript, 2002) algorithm. However, a close inspection of the Melville et al. (submitted manuscript, 2002) algorithm reveals that it is defined only for slopes up to 0.12. Taking this into consideration by eliminating all data points with slopes larger than 0.12 from the statistics, results overall in a slightly enhanced variance reductions, as can be seen from the last column of the table. However, at some locations the SSH variance does increase when going from the *Gaspar et al.* [1994] to the Melville et al. (submitted manuscript, 2002) algorithm.

[28] To investigate the effect of the EM bias correction on the high-frequency SSH variability only, we show in Table 3 statistics obtained from the SSH 10-day differences between repeat cycle. The difference signal shows a large positive impact of the EM bias correction. An exception can be found for buoy 41001 for which both algorithms enhance the η' variance, the Melville et al. (submitted manuscript, 2002) algorithm actually the most. At most other locations the variability in η' is reduced, sometimes by as much as 10%.

4. WAM Results

[29] Results from the buoy data indicate that the utilization of new algorithms for the computation of EM bias could provide more accurate estimates of SSH than currently available using project-provided EM bias corrections. However, information about wave slope and wave age, required as input, are not readily available from any satellite simultaneous with the altimeter measurements. Currently the only viable source for those fields are models, such as WAM, a wave model that was initially developed in the 1980s by an international group of modelers [*Komen et al.*, 1994].

[30] At the European Centre for Medium-Range Weather Forecasts (ECMWF), WAM has been implemented for both regional applications and the global ocean. For global applications, since December 2000 the computed spectrum has 30 frequency bins and 24 directional bins with a spatial resolution of 55 km. Analyses are produced every 6 hours. We computed the wave slopes and wave ages from the wave model output at the buoy locations for the period July 1998 to November 2000. For this period, the spectrum had only 25 frequency bins and 12 directions. For the following application, wave slope and wave age parameters were computed from the WAM output in exactly the same way as described above for the buoy data. The associated EM bias correction was applied to the altimeter data at the buoy

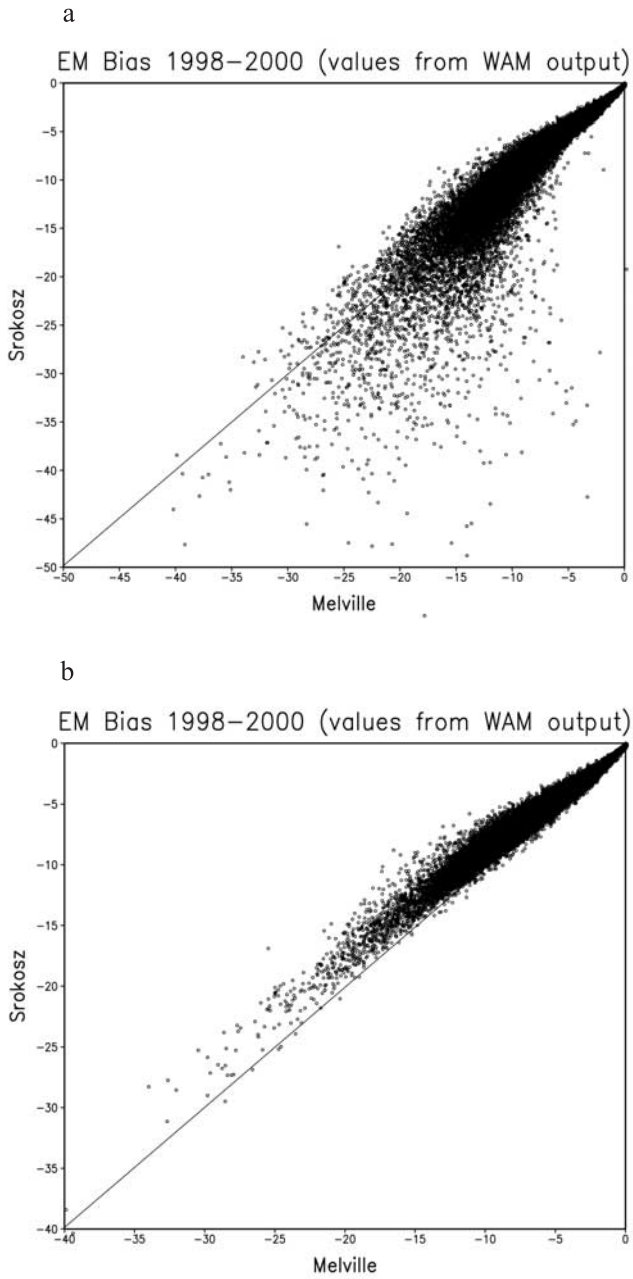

Figure 8. (a) Scatter diagram of the *Srokosz* [1986] EM bias correction versus the *Melville et al.* [1991] algorithm, both computed from 3 years of WAM output (1998–2000). The correlation, bias, and RMS difference between both corrections are 0.935, 0.04 cm, and 1.88 cm, respectively. (b) Same as Figure 8a but only for slopes not exceeding 0.12. The correlation, bias, and RMS difference between both corrections are 0.986, 0.48 cm, and 0.93 cm, respectively.

locations and compared with the results based on buoy data (see also Table 4).

[31] The availability of modeled two-dimensional frequency spectra and local winds allows a comparison of the wave slope-based empirical fit of the EM bias correction by Melville et al. (submitted manuscript, 2002) with the theoretical estimate by *Srokosz* [1986] (for alternative theoretical approaches compare *Elfouhaily et al.*, 2001]. For the period 1998 through 2000 this comparison is given in Figure 8 and shows a remarkably good agreement between the two, in particular for EM biases in the range larger than −10 cm. Taking into consideration the uncertainty of the Melville et al. (submitted manuscript, 2002) algorithm for large slopes by eliminating all data points with slopes larger than 0.12, results in a significantly increased agreement between *Srokosz* [1986] and Melville et al. (submitted manuscript, 2002) results (Figure 8b). The correlation increases from 0.935 to 0.986 and the RMS difference decreases from 1.88 cm to 0.93 cm. At the same time, the bias between both corrections changes from 0.04 cm to 0.48 cm.

[32] We note that an earlier tower-based empirical fit of *Melville et al.* [1991], which was based on significant wave height and wind speed alone, showed much less agreement with the *Srokosz* [1986] approach; for one month of data in February 1997 *Janssen* [2000] found a much larger scatter and the correlation coefficient was only 70%. Therefore these comparisons suggest a preference for a parameterization of the EM bias correction in terms of the wave slope and wave age.

[33] Under the assumption of a Gaussian shaped radar pulse, *Srokosz* [1986] obtained corrections to the waveform caused by the skewness factor λ and the slope-elevation correlation δ. For the T/P altimeter the waveform was assumed to be corrected as part of the processing for skewness effects and then only the slope-elevation correlation would be relevant (but see discussion below). The EM bias then becomes

$$\epsilon = -\frac{\delta}{8} H_{1/3} \tag{10}$$

and δ may be determined once the two-dimensional wave spectrum is known. As an illustration of the importance of the sea state, consider the example of the Phillips spectrum

$$F(k) = \frac{\alpha_p}{2} k^{-3} \tag{11}$$

with α_p being the Phillips' parameter. Then, δ becomes

$$\delta = 4\sqrt{\alpha_p}. \tag{12}$$

This illustrates the sensitive dependence of the EM bias on the sea state because the Phillips parameter may vary by a factor of 10 depending on whether the waves are wind seas or swell. For a more complete discussion see *Janssen* [2000]. The data attributed to the *Srokosz* [1986] algorithm in Figure 8 were produced by determining δ using the complete WAM spectrum.

[34] In passing, it should be pointed out that the work of *Srokosz* [1986] has been criticized on theoretical grounds by *Elfouhaily et al.* [2001]. They added effects of tilting of the short waves by the long waves and found reductions in the EM bias correction of at least 50%. The present comparison, however, does support the *Srokosz* [1986] approach [see also *Gommenginger et al.*, 2003].

[35] At many locations, slopes computed from the WAM output compare reasonably well with observed values

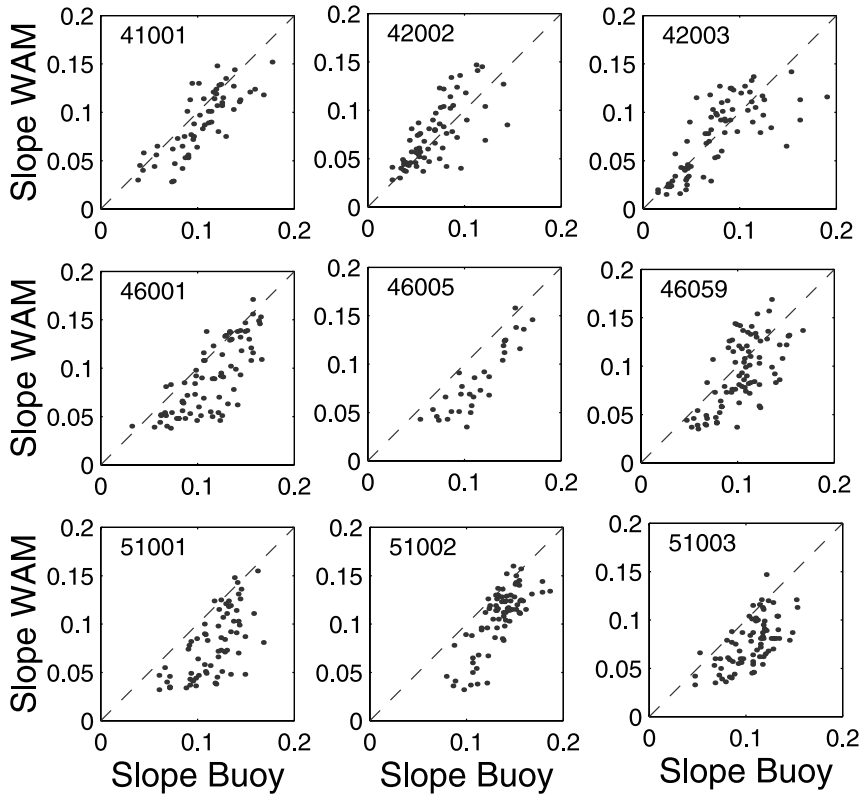

Figure 9. Scatter diagram of buoy versus WAM slopes for various buoy locations. See Table 1 for geographical buoy locations.

(Figure 9). Accordingly, WAM spectra of the wave height and waves slopes are indistinguishable from observed conditions (compare Figure 7a). However, at some locations, observed slope energy is significantly higher than WAM simulations. An explanation is given in Figure 7b which shows significant wind sea energy in the observed frequency spectra above 0.2 Hz that is not represented in the WAM results. Clearly, the details of the wave spectra at those frequencies determine the slope spectra and thus the slope computation.

[36] A summary comparison of wind speed, wave height and wave slope from all buoy locations is provided in Figure 10. Buoy wave height and T/P wind speed show high correlations between the buoy measurements and the WAM estimates, suggesting that in the absence of buoy data, WAM output should be appropriate for the purpose of EM bias computations. However, for the reasons discussed above, the agreement between measured and modeled wave slopes is not as good.

[37] Figure 11 shows a comparison of the bias corrections from WAM output and buoy data at all buoy locations using the Melville et al. (submitted manuscript, 2002) and the *Gaspar et al.* [1994] algorithms. The slope-based corrections are provided separately for slope values up to 0.2 and up to only 0.12, respectively. Bias values computed with the *Gaspar et al.* [1994] algorithm agree well with those using the Melville et al. (submitted manuscript, 2002) algorithm and buoy data for low amplitudes. However, the *Gaspar et al.* [1994] correction is biased low for high amplitudes. A similar tendency exists between WAM and *Gaspar et al.* [1994] correction; but it is less pronounced and shows more scatter. Buoy and WAM-based corrections using the Melville et al. (submitted manuscript, 2002) correction basically agree but show significant scatter. The low amplitudes of the *Gaspar et al.* [1994] correction for high amplitudes was to be expected [*Gaspar and Florens*, 1998, Figure 4b] and is an artifact of the parametric EM bias correction. (The artifact was reduced in a more recent nonparametric result as discussed by *Gaspar et al.* [2002]. However, those results were not available to us for a close inspection at the time of writing.)

[38] Table 4 illustrates that the STD of sea surface height after correcting for EM bias using the *Gaspar et al.* [1994] algorithm and the Melville et al. (submitted manuscript, 2002) algorithm decreases as was seen before, but that the WAM output leads to a slightly smaller decrease. The situation is somewhat better when slope values only up to 0.12 are used. Then the WAM output actually seems to lead to smaller SSH variances as compared to the *Gaspar et al.* [1994] correction. While interpreting these results, we need to recall that the difference between the two slope-based bias estimates using the Melville et al. (submitted manuscript, 2002) algorithm is mainly due to the difference in slope values associated with the high-frequency tail of the wave spectrum. Further improvements can be expected with an improved WAM wind sea representation and a better understanding of the small-scale wave tail. On the other hand, further improvement might be possible on the algo-

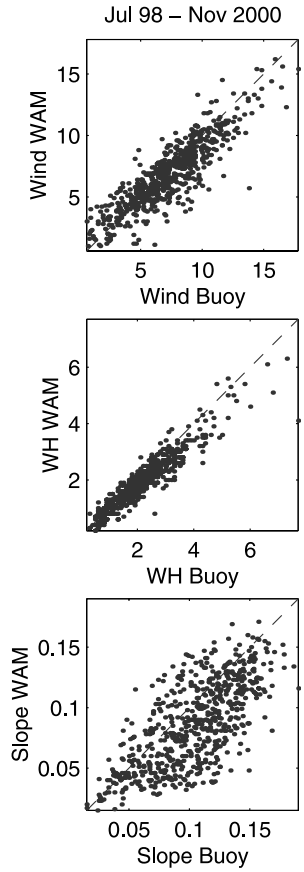

Figure 10. Scatter diagram of wave height, wind speed, and wave slope computed from all buoys and WAM output during the period July 1998 through 2000.

rithm side as well, which should include large slope amplitudes. Table 5 shows statistics similar to Table 4, but for SSH differences.

5. Discussion and Summary

[39] The EM bias correction is believed to be the source of one of the largest uncertainties in altimetric SSH observations. While this may be true for the mean EM bias, the EM bias correction appears to have a relatively small globally averaged effect on the RMS SSH variability: less than 1 cm. Reductions of SSH variance by more than 10 cm^2 seem to be confined to only a few geographic locations, notably the northern North Pacific, the subpolar North Atlantic, and upstream of Drake Passage in the South Pacific. We note that all those locations are prone to significant high-frequency barotropic variability of the ocean. Accordingly, several issues arise from our study.

[40] 1. Because empirical corrections based on satellite altimetry data are determined by minimizing the SSH or SSH difference variance signal, they will inevitably remove more than just EM bias. Here we find indications that the barotropic signal is actually leaking into empirical EM bias parameterizations. This raises the general issue of whether exclusively altimeter-based estimators [e.g., *Gaspar et al.*, 1994] can adequately represent the EM bias, or whether true ocean variability is obscured by correlations between true ocean variability and the EM bias.

[41] 2. Any approach to estimating the EM bias correction from altimeter data assumes that the covariance between SSH variability and the EM bias effect/wave signal is negligible. Here we find that the covariance is of the same magnitude than the EM bias variance itself and responsible for most of the regional pattern in the SSH variance reduction. This suggests that if such approaches are used they should be tested a posteriori to ensure that global optimization does not introduce significant regional errors.

[42] 3. To avoid this issue, empirically tested theoretical algorithms need to be developed [e.g., *Srokosz*, 1986; *Elfouhaily et al.*, 2001]. However, a full understanding of electromagnetic scattering at the ocean surface (and therefore EM bias) is lacking, due mainly to our poor knowledge of the high-wave number/high-frequency tail of the surface wave spectrum. Algorithms like the Melville et al. (submitted manuscript, 2002) parameterization are tower-based (i.e., independent of satellite altimetry) and determined from local data. This work shows significant agreement between the theoretical model of Srokosz and the tower-based measurements and algorithms as shown above. Although they need further improvement, especially on slopes larger than 0.12, i.e., outside the Bass Strait measurement range, continuing parallel development of theoretical models and in situ observations of EM bias will likely be required.

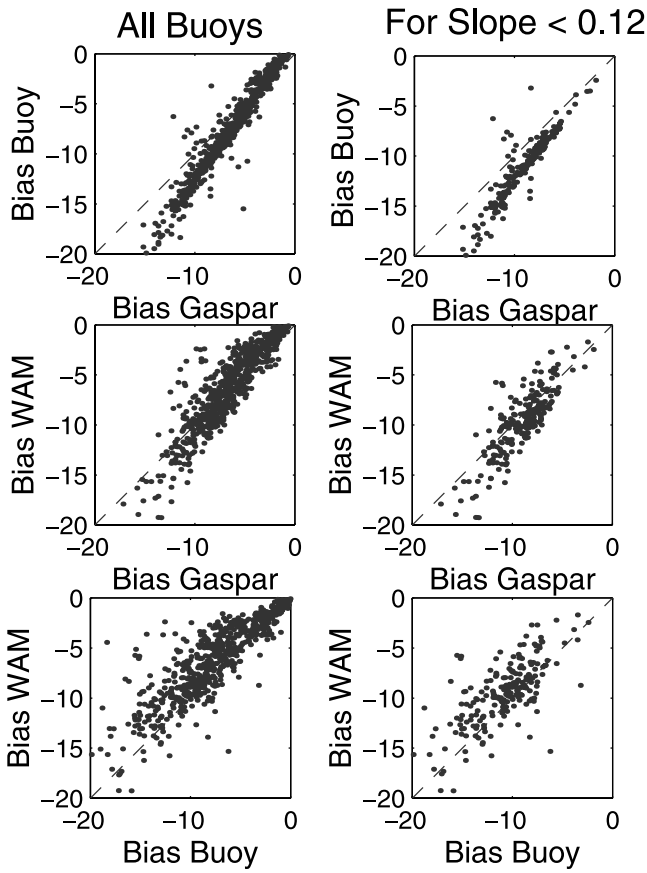

Figure 11. Scatter diagrams of EM bias corrections for (left) slopes < 0.2 and (right) slopes < 0.12.

Table 5. Standard Deviation of SSH Differences Between Successive Repeat Cycles for Slopes up to 0.2[a]

Buoy ID	Longitude, deg	Latitude, deg	Distance, m	No Pts	STD, cm				Var Diff, cm^2	
					Orig	Gasp	Buoy	WAM	Buoy	WAM
41001	287.36	34.68	0.381	15	12.2	12.4	13.1	13.4	−18.3	−25.7
42002	266.43	25.89	0.402	16	11.0	10.3	10.1	10.5	4.6	−2.8
42003	274.09	25.94	0.380	22	24.4	24.5	24.5	24.8	0.6	−18.9
46001	211.82	56.29	0.292	35	8.6	6.5	6.8	6.5	−5.1	−1.1
46059	230.00	37.98	0.156	61	6.8	6.0	6.2	7.0	−1.8	−12.9
51001	197.73	23.40	0.477	17	6.9	7.8	8.0	8.6	−3.6	−13.1
51002	202.17	17.19	0.470	21	7.0	7.5	9.1	8.2	−25.3	−10.2
51003	199.19	19.14	0.141	31	8.5	8.8	8.7	8.9	1.6	−1.6

[a]Column 5 lists the number of valid data pairs used. Columns 6–9 list the SSH standard deviation obtained without EM bias correction, when applying the *Gaspar et al.* [1994] algorithm and with the Melville et al. (submitted manuscript, 2002) algorithm separately for buoy data and WAM output. The last two columns show the reduction in SSH variance using the Melville et al. (submitted manuscript, 2002) algorithm as opposed to the *Gaspar et al.* [1994] algorithm separately for buoy data and WAM output. Positive values indicate an improvement (in cm^2).

[43] 4. WAM model output is becoming useful for EM bias corrections using both theoretical and tower-based algorithms. Again, it is in the prediction of the high-wave number region of the spectrum that the wave model needs improvement. However, direct observations of wave slope in this region of the spectrum are difficult too, and estimates of slope based on time series data are contaminated by the effects of the orbital motion of the longer waves. This gives an overestimate of spectral levels and therefore of the slope [e.g., *Banner*, 1990]. Both effects need to be taken into account when evaluating slope-based algorithms.

[44] 5. Unless there is a fundamental mechanism that is not understood for this correction of the time-varying SSH component, the largest significance of the EM bias correction is for the mean SSH correction rather than the time varying part. This will be important especially for geoid determination and to some extent for mean currents.

[45] Since this work had started, several papers have been submitted that deal with related aspects of the prediction and parameterization of EM bias. Using both the Bass Strait data (Melville et al., submitted manuscript, 2002) and the earlier tower data from the Gulf of Mexico, [*Arnold et al.*, 1995], *Millet et al.* [2003a] found improvements in EM bias parameterizations using combinations of wave slope, wind speed, and wave height, with reductions in RMS errors similar to those found by Melville et al. (submitted manuscript, 2002). However, the use of mixed dimensional and nondimensional variables is open to the same criticism of dimensional inhomogeneity as are the traditional correlations based on wind speed and wave height alone. *Millet et al.* [2003b] found that nonparametric estimates of EM bias based on the same variables led to modest improvements over traditional parameterizations. They also found strong correlations between the tower-based EM bias measurements and altimeter-derived estimates [*Gaspar and Florens*, 1998]. *Gommenginger et al.* [2003] investigated the applicability of theoretical models of EM bias by *Srokosz* [1986] and *Elfouhaily et al.* [2001] using WAM wave model data, buoy and TOPEX data. They found that the *Srokosz* [1986] model using WAM output displayed a quasi-linear correlation with the RMS wave slope, which was an improvement over traditional empirical models based on wind speed and wave height. They also found that the *Elfouhaily et al.* [2001] model was very sensitive to the high-frequency tail of the surface wave spectrum. In general, good agreement was found between the predictions of the *Srokosz* [1986] model and empirical parameterizations based on the data of Melville et al. (submitted manuscript, 2002) and the Bass Strait data (Melville et al., submitted manuscript, 2002), when using buoy and TOPEX data as input to the model and parameterizations. With this series of results there appears to be a growing consensus that the traditional parameterizations of EM bias based simply on wind speed and wave height that can be inferred from the altimeter measurements, do not faithfully represent EM bias.

[46] As noted before, a fundamental problem with evaluating EM bias algorithms is to find a measure of goodness. Ideally one needs to have in situ wave and accurate in situ SSH measurements available at the same location and over a long period of time. Moreover, such measurements should be made in several dynamically distinct regions. A number of issues need to be understood, including the interaction of the EM pulse with the surface wave field, the interaction of the wave field with the flow field, and the impact of the wind forcing on both SSH and SWH measurements. However, few field measurements are available today to address these issues. In particular, tide gauge measurements simultaneous and collocated with buoy measurements of surface waves and currents over long times are not available. In order to acquire a broad range of environmental parameters, a full suite of measurements needs to be made in high latitudes (e.g., ACC and North Pacific). It is important to explore the relative significance of the EM bias correction on the mean and the variance of the SSH, and its regional variability. From this work it appears that the differences between the EM algorithms for estimating the global variance in T/P (side A) SSH measurements are relatively small and a simple 1–2% of SWH might suffice for the T/P data. However, this work also shows that regional differences may be important and a full exploitation of altimetry for oceanographic applications will require an improved fundamental understanding of EM bias and its correlation with other oceanographic variables.

[47] It should be mentioned that EM bias corrections are frequency dependent and are different for Ku and C bands. As pointed out by a referee, theoretical approaches such as that of *Srokosz* [1986] are tested or tuned against T/P Ku band data and do not account for frequency dependency. The tower-based measurements by Melville et al. (submitted manuscript, 2002) were likewise derived for the Ku band. Furthermore, recent lessons learned from T/P and JASON revealed a significant dependence of the tracker

bias on the actual instrument. It was thought to be small for TOPEX, but could be of the order of 5% of significant wave height for other altimeters, even for the T/P side B altimeter. The problem of correcting EM bias is likely to be more complex than indicated in our study here which focuses on T/P data (a possible difference between side A and side B tracker bias was accounted for by an appropriate bias correction in the data processing procedure). For continuity of data between TOPEX and JASON 1 this is a key issue.

[48] **Acknowledgments.** Raj Kumar acknowledges the hospitality and support of the Scripps Institution of Oceanography where he spent a 15-month research visit. The comments of an anonymous referee helped significantly to improve the manuscript. Supported in part by grant NAG5-8901 from the National Aeronautics and Space Administration, and a contract with the Jet Propulsion Laboratory (1205624), both to DS, and a grant (OCE 9812182) from the National Science Foundation to WKM.

References

Arnold, D. V., W. K. Melville, R. H. Stewart, J. A. Kong, W. C. Keller, and E. Lamarre, Measurements of electromagnetic bias at Ku and C bands, *J. Geophys. Res.*, *100*, 969–980, 1995.

Banner, M. L., Equilibrium spectra of wind waves, *J. Phys. Oceanogr.*, *20*, 966–984, 1990.

Chelton, D. B., J. C. Ries, B. J. Haines, L.-L. Fu, and P. S. Callahan, Satellite altimetry, in *Satellite Altimetry and Earth Sciences*, edited by L.-L. Fu and A. Cazenave, p. 1–131, Academic, San Diego, Calif., 2001.

Cox, C., and W. H. Munk, Slopes of the sea surface deduced from photographs of sun glitter, *Bull. Scripps Inst. Oceanogr.*, *6*, 401–488, 1956.

Elfouhaily, T., D. R. Thompson, B. Chapron, and D. Vandemark, Improved electromagnetic bias theory: Inclusion of hydrodynamic modulations, *J. Geophys. Res.*, *106*, 4655–4664, 2001.

Gaspar, P., and J. P. Florens, Estimation of the sea state bias in radar altimeter measurements of sea level: Results from a new non-parametric method, *J. Geophys. Res.*, *103*, 15,803–15,814, 1998.

Gaspar, F. P., F. Ogor, P. Y. LeTraon, and O. Z. Zanife, Estimating the sea state bias of the TOPEX and Poseidon altimeters from crossover differences, *J. Geophys. Res.*, *99*, 24,981–24,994, 1994.

Gaspar, P., S. Labroue, F. Ogor, G. Lafitte, L. Marchal, and M. Rafanel, Improving nonparametric estimates of sea state bias in radar altimeter measurements of sea level, *J. Atmos. Oceanic Technol.*, *19*, 1690–1707, 2002.

Gommenginger, C. P., M. A. Srokosz, J. Wolf, and P. A. E. M. Janssen, An investigation of altimeter sea state bias theories, *J. Geophys. Res.*, *108* (C1), 3011, doi:10.1029/2001JC001174, 2003.

Hayne, G. S., D. W. Hancock, C. L. Purdy, and P. S. Callahan, The correction of significant wave height and attitude effects in the TOPEX radar altimeter, *J. Geophys. Res.*, *99*, 24,941–24,955, 1994.

Hevizi, J. G., E. Walsh, R. E. McIntosh, D. Vandemark, D. E. Hines, R. N. Swift, and J. F. Scott, Electromagnetic bias in sea surface range measurements at frequencies of the TOPEX/Poseidon satellite, *IEEE Trans. Geosci. Remote Sens.*, *31*, 376–388, 1993.

Janssen, P. A. E. M., ECMWF wave modeling and satellite altimeter wave data, in *Satellites, Oceanography and Society*, edited by D. Halpern, pp. 35–56, Elsevier Sci., New York, 2000.

Komen, G. J., L. Cavaleri, M. Donelan, K. Hasselmann, S. Hasselmann, and P. A. E. M. Janssen, *Dynamics and Modeling of Ocean Waves*, 1st ed., 532 pp., Cambridge Univ. Press, New York, 1994.

Melville, W. K., R. H. Stewart, W. C. Keller, J. A. Kong, D. V. Arnold, A. T. Jessup, M. R. Loewen, and A. M. Slinn, Measurement of electromagnetic bias in radar altimetry, *J. Geophys. Res.*, *96*, 4915–4924, 1991.

Millet, F. W., D. Arnold, K. Warnick, and J. Smith, Electromagnetic bias estimation using in situ and satellite data: 1. RMS wave slope argument, *J. Geophys. Res.*, *108*(C2), 3040, doi:10.1029/2001JC001095, 2003a.

Millet, F. W., D. Arnold, K. Warnick, and J. Smith, Electromagnetic bias estimation using in situ and satellite data: 2. A nonparametric approach, *J. Geophys. Res.*, *108*(C2), 3041, doi:10.1029/2001JC001144, 2003b.

Mitchum, G., Comparison of TOPEX sea surface heights and tide gauge sea levels, *J. Geophys. Res.*, *99*, 24,541–24,543, 1994.

Ponte, R., and P. Gaspar, Regional analysis of the inverted barometer effect over the global ocean using TOPEX/Poseidon data and model results, *J. Geophys. Res.*, *104*, 15,587–15,602, 1999.

Ray, R. D., and C. J. Koblinsky, On the sea-state bias of the Geosat altimeter, *J. Atmos. Oceanic Technol.*, *8*, 397–408, 1991.

Srokosz, M. A., On the joint distribution of surface elevation and slope for a nonlinear random sea, with application to radar altimetry, *J. Geophys. Res.*, *91*, 995–1006, 1986.

Stammer, D., and C. Wunsch, Preliminary assessment of the accuracy and precision of TOPEX/Poseidon altimeter data with respect to the large scale ocean circulation, *J. Geophys. Res.*, *99*, 24,584–25,604, 1994.

Stammer, D., C. Wunsch, and R. Ponte, De-aliasing of global high frequency barotropic motions in altimeter observations, *Geophys. Res. Lett.*, *27*, 1175–1178, 2000.

Yaplee, B., A. Shapiro, D. Hammond, B. Au, and E. Uliana, Nanosecond radar observations of the ocean surface from a stable platform, *IEEE Trans. Geosci. Electron.*, *9*, 170–174, 1971.

P. Janssen, European Centre for Medium-Range Weather Forecasts, Shinfield Park, Reading RG2 9AX, UK.

R. Kumar, Oceanic Sciences Division, MOG/RESA, Space Applications Centre (ISRO), Ahmedabad 380 015, India.

W. K. Melville and D. Stammer, Scripps Institution of Oceanography, 9500 Gilman Drive, La Jolla, 92093-0230 CA, USA. (dstammer@ucsd.edu)